Development 122, 2997-3011 (1996)
Printed in Great Britain © The Company of Biologists Limited 1996
DEV2094

Hoxa-13 and *Hoxd-13* play a crucial role in the patterning of the limb autopod

Catherine Fromental-Ramain†, Xavier Warot†, Nadia Messadecq, Marianne LeMeur, Pascal Dollé and Pierre Chambon*

Institut de Génétique et de Biologie Moléculaire et Cellulaire, CNRS/INSERM/ULP, Collège de France, BP 163-67404 ILLKIRCH-CEDEX, C. U. de Strasbourg, FRANCE

*Author for correspondence
†Should be considered as equal first author

SUMMARY

Members of the *Abdominal-B*-related *Hox* gene subfamily (belonging to homology groups 9 to 13) are coordinately expressed during limb bud development. Only two genes from homology group 13 (*Hoxa-13* and *Hoxd-13*) are specifically expressed in the developing distal region (the autopod), which displays the most complex and evolutionarily flexible pattern among limb 'segments'. We report here that targeted disruption of the *Hoxa-13* gene leads to a specific forelimb and hindlimb autopodal phenotype, distinct from that of the *Hoxd-13* paralogous gene inactivation. In both limbs, *Hoxa-13* loss of function results in the lack of formation of the most anterior digit and to altered morphogenesis of some 'preaxial' carpal/tarsal elements. We have generated mice with all possible combinations of disrupted *Hoxa-13* and/or *Hoxd-13* alleles, which allowed us to investigate the degree of functional specificity versus redundancy of the corresponding gene products in the developing limb autopod. The phenotype of any double mutant was much more severe than the sum of the phenotypes seen in the corresponding single mutants, indicating that these genes act in a partially redundant manner. Our major findings were: (1) an abnormal autopodal phenotype in *Hoxa-13*$^{+/-}$/*Hoxd-13*$^{+/-}$ double heterozygous mutants, which mostly consists of subsets of the alterations seen in each individual homozygous mutant, and therefore appears to result from quantitative, rather than qualitative, homeoprotein deficiency; (2) partly distinct alterations in mutants harboring a single non-disrupted allele of *Hoxa-13* or *Hoxd-13*, indicating that the remaining reduced protein amounts are not functionally equivalent; (3) a polydactyly in the forelimbs of *Hoxa-13*$^{+/-}$/*Hoxd-13*$^{-/-}$ double mutants, consisting of seven symmetrically arranged, truncated and mostly non-segmented digits; (4) an almost complete lack of chondrified condensations in the autopods of double homozygous mutants, showing that the activity of group 13 Hox gene products is essential for autopodal patterning in tetrapod limbs.

Key words: *Hox-13*, patterning, autopod, gene disruption, mouse, limb, digit formation

INTRODUCTION

The vertebrate limb bud is an excellent system for studying the cellular and molecular mechanisms of pattern formation. Limb buds arise from the lateral plate mesoderm and their outgrowth is maintained by the influence of an apical ectodermal ridge (AER). During recent years, several signaling molecules, which provide growth and/or patterning information along the three major limb axes, have been identified. The fibroblast growth factors FGF-4 and FGF-8, produced by the AER, are involved in proximodistal limb bud growth (Crossley et al., 1996 and refs therein). Sonic hedgehog and the bone morphogenetic protein BMP-2 appear to mediate the signaling properties of the posterior polarizing region (Riddle et al., 1993; Francis et al., 1994), whereas the Wnt-7a gene product released by the dorsal ectoderm is implicated in dorsoventral patterning (Parr and McMahon, 1995). Unraveling the molecular events triggered by such factors and how these events lead to the generation of morphological pattern is the goal of current research.

The limb pattern is believed to be determined in the chondrogenic (preskeletal) cell lineage (Hinchliffe and Johnson, 1980 and refs therein). Mesenchymal cells of the limb bud first aggregate to form a central prechondrogenic condensation or blastema. This condensation grows by aggregation of additional mesenchymal cells at its distal end (Archer et al., 1984). As the three regions of the limb become distinct (the stylopod, zeugopod and autopod from proximal to distal), a preskeletal pattern is generated by sequential dichotomous branching of the primary condensation (Shubin and Alberch, 1986). A first branching event generates two zeugopodal elements (the radius/ulna or tibia/fibula anlagen) from the proximal stylopodal condensation (the humerus or femur anlage). Additional branching events will generate the various elements of the autopods (the carpal/tarsal and digit cartilages). The final skeletal pattern also depends on segmentation events leading to the formation of distinct cartilages from a single chondrogenic condensation. For instance, all digit phalanges are generated by segmentation of primary metacarpal/metatarsal condensations. The sequence of branching and segmentation events appears to be highly conserved across species and may be considered as a 'bauplan' (conserved pattern of morphological organization) of the tetrapod limb (Shubin, 1991). Mor-

phological variability between species results from the absence of some branching events, absence of chondrification or ossification, differential growth or secondary fusions between condensations (Müller, 1991).

Members of the *Hox* gene family are believed to regulate pattern formation in the developing limbs. The murine genome contains 38 *Hox* genes phylogenetically related to *Drosophila* homeotic genes and clustered in four chromosomal loci, the *HoxA, B, C* and *D* complexes (McGinnis and Krumlauf, 1992; Dollé and Duboule, 1993 and refs therein). *Hox* genes encode homeodomain proteins, which have been shown to act as transcriptional regulators (e.g. Zappavigna et al., 1994), although most of their target DNA-binding sites are still unknown. A 5′ to 3′ orientation can be assigned to each complex according to the common direction of transcription of all of its members. The *Hox* family can be divided in 13 groups of highly related paralogous genes, which have the same relative position in their respective complex. All *Hox* genes display restricted expression domains along the embryo rostrocaudal axis and their rostral expression boundaries are correlated with the chromosomal location of the genes (Graham et al., 1989; Duboule and Dollé, 1989). Genes located at the 5′ extremity of the *HoxA* and *HoxD* complexes (belonging to homology groups 9 to 13 and related to the *Drosophila Abdominal-B* gene) are, in addition, coordinately expressed in the developing limbs. Their sequential (3′ to 5′) activation during early limb budding leads to colinear and nested transcript domains. Thus, at early stages, *Hoxa-13* and *Hoxd-13* display the most restricted expression domains toward the posterior and distal region of the limb bud or polarizing region (Dollé et al., 1989; Yokouchi et al., 1991; Haack and Gruss, 1993). At later stages, the *Hoxd-11, d-12* and *d-13* genes are activated distally in the entire autopod (Duboule, 1994 and refs therein). *Hoxa-13*, but not *Hoxa-11*, is similarly expressed in the whole autopod region (Haack and Gruss, 1993). While the posterior colinear expression appears to have predated the evolutionary fin/limb bud transition, the secondary expression phase has no counterpart in the teleost fin bud, and has been proposed to have evolved in the tetrapod lineage to allow the formation of complex autopodal derivatives (the tetrapod feet; Sordino et al., 1995; Coates, 1995).

Gene ‘knockout’ studies in mice (Dollé et al., 1993; Small and Potter, 1993; Davis and Capecchi, 1994; Favier et al., 1995, 1996; Fromental-Ramain et al., 1996) and misexpression experiments in chick embryos (Morgan et al., 1992; Yokouchi et al., 1995) have shown that various *Hoxa* and *Hoxd Abdominal-B*-related genes are functional in the developing limbs. The loss-of-function phenotypes consist of truncations or fusions of specific skeletal elements rather than morphological transformations. The *Hoxd-13*$^{-/-}$ targeted mutation results in severe growth retardation of various autopodal cartilages and selective lack of cartilages that are the last to develop in wild-type (WT) mice (Dollé et al., 1993). It was therefore proposed that this mutation induces localized heterochrony (a reduction of the growth rate of the autopod skeleton) leading to adult neotenic limbs (displaying fetal traits). To further investigate the function of *Hox* genes in the developing autopod, we have now disrupted the *Hoxa-13* gene. Here, we describe and discuss the limb phenotype of *Hoxa-13* loss-of-function mutants, as well as compound mutants with various combinations of disrupted *Hoxa-13* and/or *Hoxd-13* alleles.

MATERIALS AND METHODS

Construction of *Hoxa-13* targeting vectors

Disruption of the *Hoxa-13* homeobox by insertion of a neo^r gene

A 2.6 kb *Hin*dIII 129/SV genomic fragment containing the *Hoxa-13* homeobox and 3′ untranslated sequences was subcloned into the pTZ plasmid (Pharmacia). The neo^r gene driven by a thymidine kinase (TK) promoter was excised from the pMC1neo plasmid (Thomas and Capecchi, 1987; a gift from M. Capecchi), blunt-ended and ligated into the *Eco*RV site of the homeobox, yielding the pTZHVneo construct. In parallel, a 3 kb *Xho*I-*Hin*dIII genomic fragment corresponding to the 5′-flanking region of the homeobox-containing *Hin*dIII fragment, was subcloned in pBluescriptSK (Stratagene), yielding the pSKXH construct. In a second step, the TK cassette from plasmid pD352 (a gift from D. Lohnes; Rijli et al., 1994) was inserted in pSKXH at the 5′ extremity of the genomic fragment, leading to the pTKXH construct. Finally, the *Hin*dIII fragment from pTZHVneo was inserted in the *Hin*dIII site of pTKXH to obtain the pTKa-13MC1neo targeting vector. This construction generates a disruption of the Hoxa-13 protein sequence at the level of the 34th amino acid (i.e. in the middle of the second α-helix) of the homeodomain. The targeting vector was linearized by *Kpn*I prior to electroporation of ES cells.

Deletion of the *Hoxa-13* gene and replacement by the neo^r gene

The 3 kb *Xho*I-*Hin*dIII and 2.6 kb *Hin*dIII-*Hin*dIII genomic fragments described above were subcloned adjacently in the pSL1190 (*Xba*I$^-$) plasmid (Pharmacia), yielding the pSLXHH construct. This plasmid was digested by *Xba*I, blunt ended and ligated to the neo^r gene from pMC1neo (Thomas and Cappechi, 1987), leading to the pXHΔneo plasmid. The *Xba*I digestion generated a 2.8 kb deletion. Since the 3′ *Xba*I site was located downstream of the second exon (480 bp from the acceptor splice site), this deletion encompassed the second exon, the intron and the first exon (Mortlock et al., 1996). A 1.6 kb *Spe*I-*Xho*I genomic fragment, corresponding to the 5′-flanking region of the *Xho*I-*Hin*dIII fragment, was then added to pXHΔneo, leading to the pSHΔneo plasmid. Finally, the whole genomic fragment excised from pSHΔneo was subcloned upstream of the diphteria toxin gene into the pJB101DT plasmid (McCarrick III et al., 1993), to obtain the pDTa-13ΔMC1neo targeting construct. The vector was linearized by *Hin*dIII before electroporation of ES cells.

Identification of the targeted ES cell clones

Electroporations and ES cell culture were performed as described (Dollé et al., 1993) and targeted clones were identified by Southern blot analysis. Two electroporation experiments of 15×10^6 D3 ES cells (Gossler et al., 1986) were performed with the pTKa-13MC1neo construct and each resulted in one targeted ES cell clone out of 84 and 83 G418/Gancyclovir resistant clones. Electroporation of 9×10^6 H1 cells (an ES cell line established in our laboratory) with the pDTa-13ΔMC1neo construct resulted in three targeted clones out of 100 G418 resistant clones.

The probes used for Southern blot analysis were as follows. In the case of the pTKa-13MC1neo construct, the 5′-external probe A (a 600 bp *Eco*RI-*Xho*I fragment) hybridized to a 5.5 kb WT and a 4.5 kb mutated allele upon *Eco*RI digestion of ES cell genomic DNA. The 3′ external probe B (a 900 bp *Bgl*II-*Nde*I fragment) hybridized to a 12 kb WT and a 9 kb mutated allele upon *Bam*HI digestion. In the case of the pDTa-13ΔMC1neo construct, the 5′ external probe C (a 720 bp *Eco*RI-*Eco*RI fragment) hybridized to a 7.1 kb WT and a 7.8 kb mutated allele upon *Hin*dIII digestion. The 3′ external probe B recognized a 12 kb WT and a 8.7 kb mutated allele upon *Bam*HI digestion. A neomycin probe was also used in all cases to discriminate ES cell clones containing random insertion of the plasmid.

Establishment of the mutant mouse lines

Upon injection into C57Bl/6 blastocysts, four independent targeted ES cell clones (two for each mutation described above) yielded germline-transmitting male chimeras. These chimeras were crossed with C57Bl/6 or 129/SV females to produce heterozygous mutants in mixed (129/SV-C57Bl/6) or inbred (129/SV) genetic backgrounds. Heterozygous mutants were intercrossed to generate homozygous mutant fetuses. Southern blot analysis of tail tip or extra-embryonic membrane DNA was performed using probe B described above.

The *Hoxd-13* mutant line has been described previously (Dollé et al., 1993). *Hoxa-13*$^{+/-}$ heterozygotes (harboring the homeodomain insertional mutation) were crossed to *Hoxd-13*$^{+/-}$ mutants to generate double heterozygous mutants. These double heterozygotes were intercrossed to obtain the various compound mutant genotypes.

Skeletal analyses

The alizarin red-alcian blue skeletal staining procedure for newborn and adult animals has been previously described (Dollé et al., 1993) and the whole-mount fetal alcian blue stainings were carried out on fetuses from day 10.5 to day 16.5 post-coitum (dpc), as described in Jegalian and De Robertis (1992).

Scanning electron microscopy

Embryos were fixed overnight at 4°C in 2.5% glutaraldehyde in 0.1 M cacodylate buffer (pH 7.2) and washed in cacodylate buffer for 30 minutes. After postfixation with 1% OsO_4 in 0.1 M cacodylate buffer (1 hour at 4°C), the embryos were dehydrated by an ascending ethanol series and dried by the critical point method, coated with conducting carbon glue, sputtered-coated with palladium-gold and examined with a Philips XL20 scanning electron microscope.

RESULTS

Hoxa-13$^{-/-}$ mutant fetuses exhibit an abnormal autopodal phenotype

Two targeted disruptions of the *Hoxa-13* gene were generated in ES cells: in one of them, a selectable marker disrupts the homeobox sequence and in the other, the selectable marker replaces 2.8 kb of genomic DNA, which includes both exons and the intron of *Hoxa-13* (see Materials and methods). Both targeted mutations produced the same phenotype. While *Hoxa-13*$^{+/-}$ heterozygous mutants were viable, fertile and displayed only minor limb abnormalities (see below), no *Hoxa-13*$^{-/-}$ homozygous mutant could be recovered post-partum or in 18.5 dpc litters delivered by caesarean section (Table 1). Earlier sample collection showed that *Hoxa-13*$^{-/-}$ mutants died between 11.5 and 15.5 dpc. At each of these developmental stages, a fraction of the *Hoxa-13*$^{-/-}$ mutant fetuses were found dead (Table 1), while the living homozygous mutants did not exhibit any obvious external abnormalities except at the level

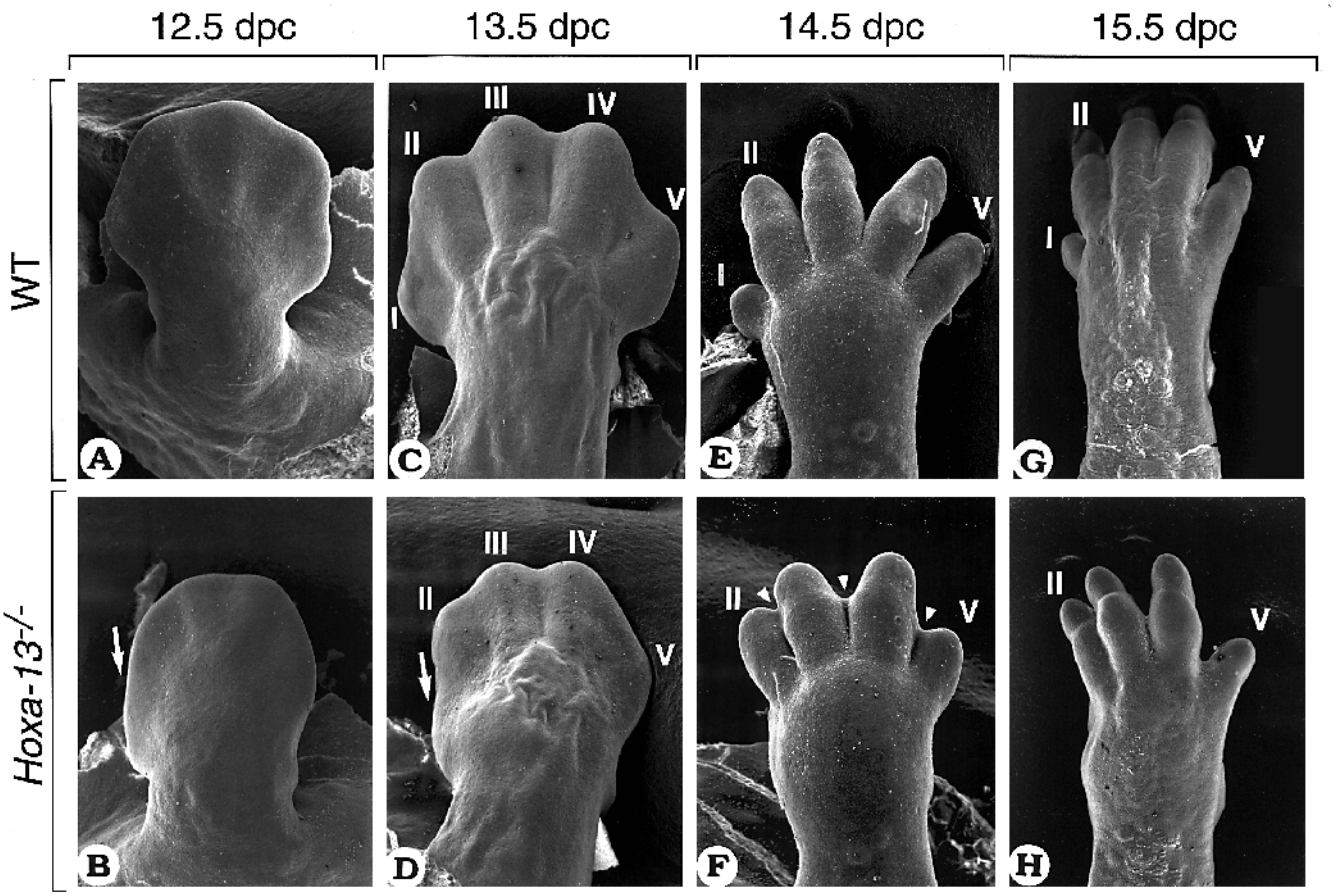

Fig. 1. Scanning electron micrographs of the forelimb extremities of WT (A,C,E,G) and *Hoxa-13*$^{-/-}$ (B,D,F,H) fetuses at various developmental stages (as indicated above), viewed from their dorsal aspects. The arrows in B and D point to the abnormally flat anterior margin of the mutant footplates, from which no digit I protrusion will appear at later stages. The arrowheads in F indicate the poor digit separation in 14.5 dpc mutants. Digits are numbered with roman numerals.

Table 1. Lethality of *Hoxa-13*$^{-/-}$ embryos during development

Genotype	Age (dpc)							
	10.5	11.5	12.5	13.5	14.5	15.5	16.5	18.5
+/+	17	31	36	29	19	21	11	22
+/–	21	56	83	51	56	39	30	43
–/–	17 (0) [0]	38 (5) [13]	30 (7) [23]	35 (14) [40]	19 (11) [58]	20 (16) [80]	2 (2) [100]	9 (9) [100]

The number of embryos or fetuses recovered is indicated for each genotype at different developmental stages. At each stage the number of dead *Hoxa-13*$^{-/-}$ embryos or fetuses and their frequency (in percent) are given in parenthesis and brackets, respectively. The Mendelian ratios are respected until 15.5 dpc. At later stages the majority of the dead embryos were resorbed and their genotypes could not be determined.

of the limbs (see below). The cause of the fetal lethality is presently under investigation.

The external morphology of *Hoxa-1*$^{-/-}$ developing limbs was analyzed by scanning electron microscopy. Similar fully penetrant alterations were detected in forelimbs and hindlimbs and are shown here for the forelimbs only (Fig. 1). Abnormalities of the limb extremities were seen as early as 12.5 dpc. At that stage, the footplates of *Hoxa-13*$^{-/-}$ mutants were narrower that those of WT and were abnormally flat along their anterior margin (Fig. 1A,B). This early phenotype might, in part, correspond to a developmental delay of mutant limb autopods. However, examination of later stages revealed persistent alterations which cannot be explained solely by a developmental retardation. At 13.5 dpc, the mutant footplates were still narrower than their WT counterparts and showed only four digit anlagen (Fig. 1C,D). There was no well-defined protrusion corresponding to digit I, whereas this digit primordium was already seen in 12.5 dpc WT limbs (Fig. 1A,D). At 14.5 dpc, digit I was clearly absent in the mutants and the other digits were not properly separated (Fig. 1E,F). Digit I was still

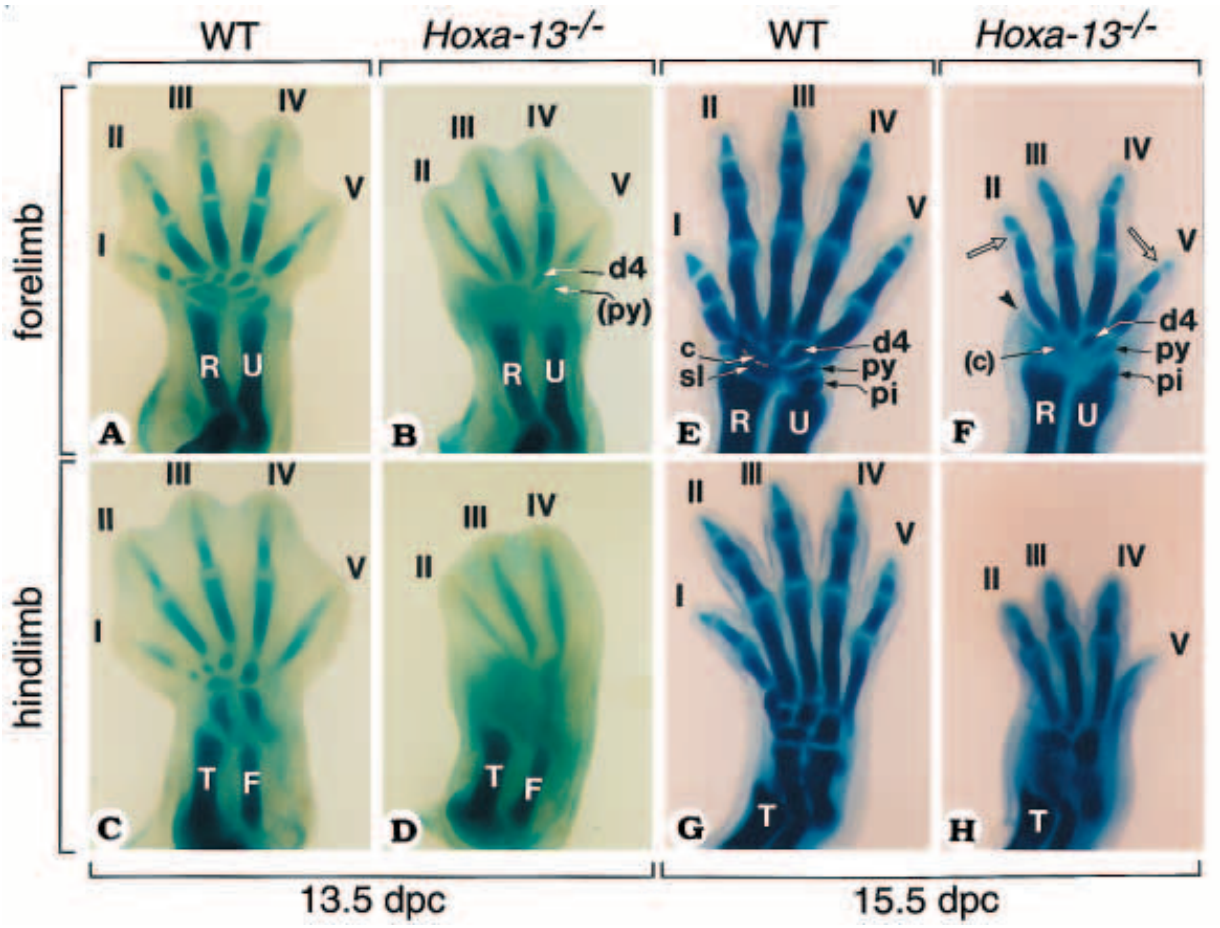

Fig. 2. Comparison of the limb chondrogenic patterns of WT (A,C,E,G) and *Hoxa-13*$^{-/-}$ (B,D,F,H) fetuses at 13.5 dpc (A-D) and 15.5 dpc (E-H). The fetal limbs were stained as whole mounts with alcian blue and are viewed from their dorsal side. The arrowhead in F shows the small condensation which may represent a digit I rudiment in the mutant forelimb, and the open arrows indicate the lack of a second phalangeal cartilage in digits II and V. C, (putative) central blastema; d4, distal carpal 4; F, fibula; pi, pisiform; py, (putative) pyramidal blastema; R, radius; sl, scapholunatum; T, tibia; U, ulna. Digits are numbered with roman numerals.

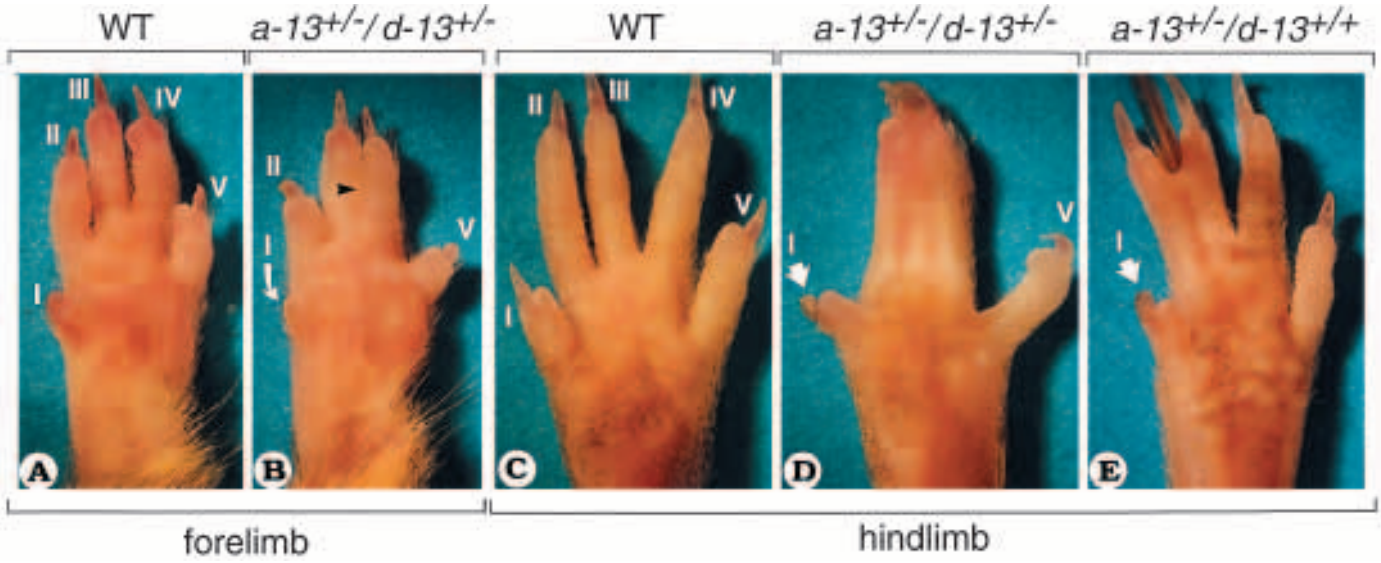

Fig. 3. Palmar views of the forepaws (A,B) and hindpaws (C-E) of WT (A,C), *Hoxa-13*$^{+/-}$*/Hoxd-13*$^{+/-}$ (B,D) and *Hoxa-13*$^{+/-}$ (E) adult (2-month-old) mice. The arrowhead in B points to the limit of the interdigital fusion between the forelimb digits II and III. Digits are numbered with roman numerals.

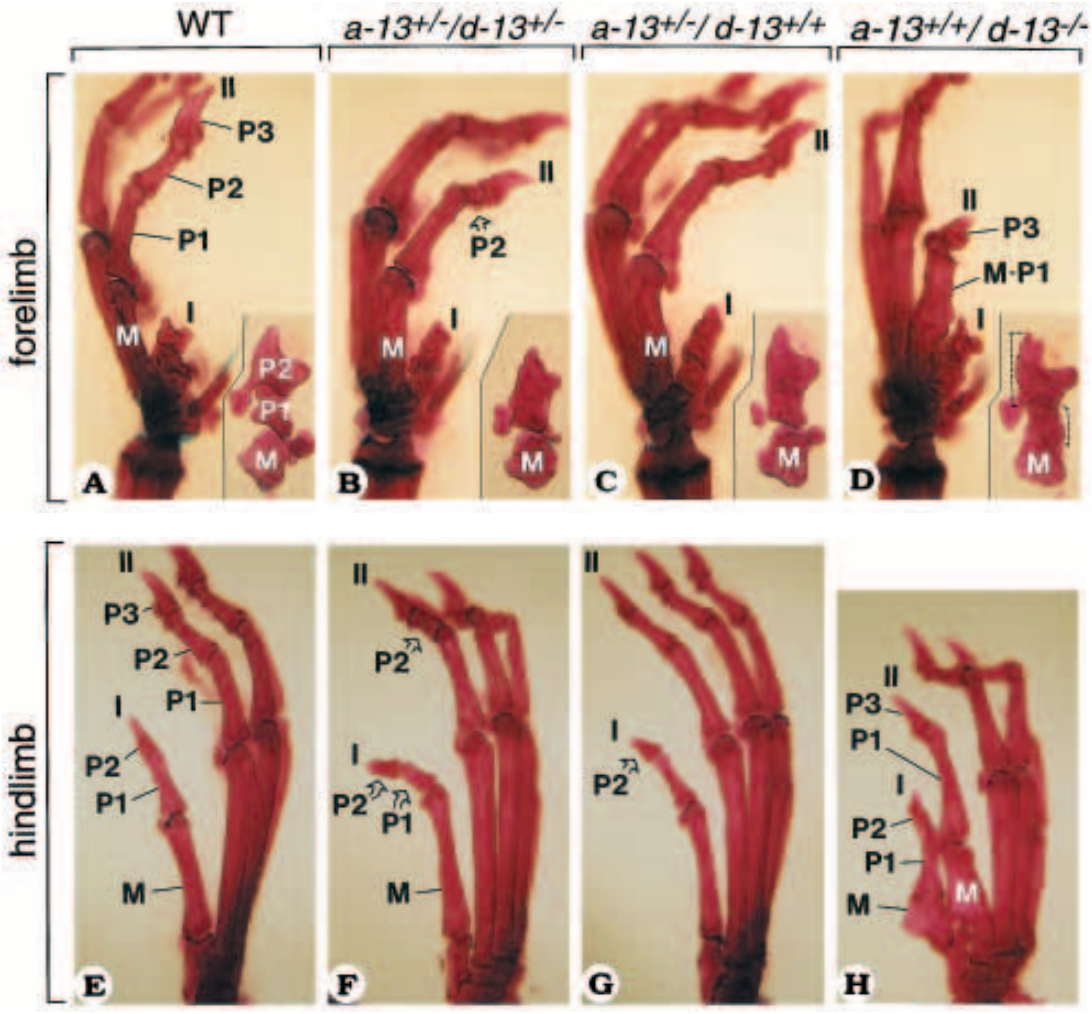

Fig. 4. Comparison of the skeletal alterations of the first and second digits of the forelimb (A-D) and hindlimb (E-H) of adult WT (A,E), *Hoxa-13*$^{+/-}$*/Hoxd-13*$^{+/-}$ (B,F), *Hoxa-13*$^{+/-}$ (C,G) and *Hoxd-13*$^{-/-}$ (D,H) mice. The inserts in A-D show an enlarged profile view of the thumbs (digits I) of the same specimens after dissection. In D, the brackets indicate the first and second phalanges of the thumb which, although fused together and to the metacarpal bone, can still be recognized. M, metacarpal or metatarsal bone; P1-P3, phalangeal bones. Digits are numbered with roman numerals.

missing at 15.5 dpc, the latest stage at which *Hoxa-13*$^{-/-}$ mutants could be analyzed (Fig. 1H). Furthermore, there was a lack of separation (webbing) between digits II and III and an abnormal bending of the digits toward the anterior side (Fig. 1G,H). Similar abnormalities were observed in hindlimb autopods which, in particular, consistently lacked digit I and exhibited an abnormal bending of digits II and III toward the anterior side at 14.5 and 15.5 dpc (data not shown).

The chondrification pattern of the preskeletal limb elements was analyzed by whole-mount alcian blue staining. At 11.5 and 12.5 dpc, mutant limbs showed no alteration of the early (stylopod, zeugopod and digital arch) chondrogenic condensations, although the initial digit condensations were delayed with respect to WT littermates (data not shown). At 13.5 dpc, mutant digits II, III and IV underwent chondrification and segmentation of their cartilages (Fig. 2B,D), but were retarded in comparison to WT specimens (Fig. 2A,C). In contrast, there was no primary condensation of digit I in both mutant forelimbs (Fig. 2B) and hindlimbs (Fig. 2D), and a small digit V condensation could be seen in mutant forelimbs only (Fig. 2B).

Examination of 14.5 and 15.5 dpc mutants showed no chondrogenic condensation for digit I in both forelimbs and hindlimbs (Fig. 2F,G and data not shown). A minute cartilage ray, which may correspond to a digit I rudiment, was observed in 15.5 dpc mutant forelimbs (Fig. 2F, arrowhead). Digit V eventually underwent proper development in the mutant forelimbs (Fig. 2F), but remained in the state of a small and thin primary condensation in the hindlimbs until 15.5 dpc (Fig. 2H). Mutant digits II, III and V of both forelimbs and hindlimbs were reduced in size, but their cartilaginous elements were well-defined and segmented (Fig. 2F,H). However, the 15.5 dpc mutant forelimb digits II and V selectively lacked the second phalangeal cartilages (Fig. 2F, open arrows). At the same stage, all mutant hindlimb digits lacked the second phalangeal cartilages (Fig. 2H).

The *Hoxa-13*$^{-/-}$ mutation also affected chondrogenesis of the carpal and tarsal elements. Whereas most of the carpal (Fig. 2A) and tarsal (Fig. 2C) cartilage models were distinctly formed in 13.5 dpc WT fetuses, *Hoxa-13*$^{-/-}$ mutants exhibited no distinct carpal condensations except for the distal carpal 4 (d4) and possibly the pyramidal (py) (Fig. 2B). No tarsal element was individualized and the hindlimb autopod still displayed an early pattern of connectivity between the fibula and digit IV (Fig. 2D). The pattern of carpal elements remained abnormal at subsequent developmental stages. At 15.5 dpc, mutants had well-defined pisiform (pi) and distal carpal 4, rudimentary pyramidal and poorly defined central and distal carpals (Fig. 2F). There was no discernable scapholunatum cartilage (sl) (Fig. 2F). At this stage, the entire mutant tarsus showed poor modeling of its elements (Fig. 2H). Note, however, that the distal extremity of the radius/ulna and tibia/fibula were normal in *Hoxa-13*$^{-/-}$ mutants.

Hoxa-13/Hoxd-13 compound heterozygotes display abnormalities found in both *Hoxa-13* and *Hoxd-13* null mutants

Double heterozygous *Hoxa-13*$^{+/-}$*/Hoxd-13*$^{+/-}$ mice were produced by intercrossing single heterozygous mutants. The compound heterozygotes, which were viable and fertile, displayed a fully penetrant phenotype in all four limb autopods. Externally, digits II and V of the adult forelimbs were clearly truncated (Fig. 3B). This phenotype was also seen in *Hoxd-13*$^{-/-}$ mutants (Dollé et al., 1993). Furthermore, the forelimb digit I, which is naturally truncated in WT mice, was even smaller in compound heterozygotes (Fig. 3B, white arrow). These animals also exhibited partial fusions between forelimb digits III and IV (Fig. 3B, arrowhead) and extensive fusions between hindlimb digits II, III and IV (Fig. 3D). In both cases these interdigital fusions (webbing) occured only at the level of soft tissues, with the phalangeal cartilages of hindlimb digits II, III and IV being almost adjacent at the level of their perichondria (not shown). Compound heterozygotes also presented deformed hindlimb digits I and V (Fig. 3D). Interestingly, two hindlimb abnormalities were consistently seen in single *Hoxa-13*$^{+/-}$ heterozygous mutants: (1) partial fusion between digits II and III (Fig. 3E), and (2) alteration of the claw of digit I (Fig. 3D,E).

Skeletal stainings of adult compound heterozygotes revealed specific alterations of both forelimb and hindlimb first digits. The WT forelimb digit I ('thumb'), while naturally truncated, displays distinct metacarpal, first and second phalangeal bones (Fig. 4A). In compound heterozygotes, this digit was exaggerately truncated and displayed no visible first phalanx (Fig. 4B). Interestingly, newborn specimens showed an incomplete segmentation between the two phalangeal cartilages of digit I (data not shown), suggesting that these two cartilages ossify together, in compound heterozygotes, to form a single truncated bone. *Hoxa-13*$^{+/-}$ single heterozygotes also displayed a fusion between the two phalanges of digit I, although these were not truncated as in compound heterozygotes (Fig. 4B,C). This abnormal phenotype is clearly distinct from that of *Hoxd-13*$^{-/-}$ mutants where all three bones of digit I, although fused together, could be identifed and were not truncated (Fig. 4D). Double heterozygous mutants also had typical alterations of the hindlimb digit I: its first phalanx (P1) was truncated and the terminal phalanx (P2) had an altered 'bell-shaped' morphology (Fig. 4F). Both phalanges of digit I were actually fused together in some specimens (data not shown). Intriguingly, the metatarsal bone of digit I was longer than in WT mice, thus 'compensating' for the phalangeal shortening (Fig. 4E,F). Note that the first digits of the hindlimb are differently affected in *Hoxa-13*$^{+/-}$*/Hoxd-13*$^{+/-}$ and in *Hoxd-13*$^{-/-}$ mutants (Fig. 4F,H, respectively). Note also that *Hoxa-13*$^{+/-}$ single heterozygotes displayed an abnormal 'bell-shape' of the terminal phalanx of digit I, but no alteration of its metatarsal or first phalangeal bone (Fig. 4G).

While *Hoxa-13*$^{+/-}$ single heterozygotes displayed no abnormalities other than those seen in the forelimb and hindlimb first digits, *Hoxa-13*$^{+/-}$*/Hoxd-13*$^{+/-}$ compound heterozygotes had additional alterations, which were reminiscent of the *Hoxd-13*$^{-/-}$ phenotype. The second phalanges (P2) of digits II were clearly truncated, both in forelimbs and hindlimbs (Fig. 4B,F). These phalanges were generally absent in *Hoxd-13*$^{-/-}$ mutants (Fig. 4D,H). Similarly, the second phalanges of digits V were absent in most compound heterozygotes, or otherwise severely truncated (Fig. 5B,C; hindlimb data not shown). The same was true for *Hoxd-13*$^{-/-}$ mutants (data not shown; Dollé et al., 1993). Many *Hoxa-13*$^{+/-}$*/Hoxd-13*$^{+/-}$ specimens (23 out of 40 limbs examined) displayed a supernumerary posterior digit rudiment in the forelimbs, consisting either of a small floating bone distal to the post-minimus (Fig. 5B, V*) or an entire small

Table 2. Summary of limb abnormalities of *Hoxa-13*$^{+/-}$, *Hoxa-13*$^{+/-}$/*Hoxd-13*$^{+/-}$ and *Hoxd-13*$^{-/-}$ adult mutant mice

	Mutant		
Limb abnormality	*Hoxa-13*$^{+/-}$	*Hoxa-13*$^{+/-}$ *Hoxd-13*$^{+/-}$	*Hoxd-13*$^{-/-}$
Forelimbs			
Metacarpal/phalangeal bone fusions	–	–	+
Truncated metacarpals	–	–	+
Missing/truncated P2 (digits II and V)	–	+	+
Sixth digit rudiment (post.)	–	(+)	(+)
Missing/truncated P1 (digit I)	(+)	+	–
Interdigital fusions (soft tissues)	–	+ (III-IV)	–
Hindlimbs			
Truncated metatarsals	–	–	+
Missing/truncated P2 (digits II and V)	–	+	+
Sixth digit (post.)	–	–	(+)
Truncated P1 (digit I)	–	+	–
Altered terminal phalanx (digit I)	+	+	–
Interdigital fusions (soft tissues)	(+) (II-III)	+ (II-III-IV)	–

+, fully penetrant abnormality; (+), incompletely penetrant or milder abnormality; –, no abnormality.
Roman numerals refer to the digits that are fused.
Post., posterior.

digit (Fig. 5C, V*). Similar sixth digit rudiments were seen in most *Hoxd-13*$^{-/-}$ mutants (Dollé et al., 1993). Interestingly, the fourth (posterior) distal carpal bone (*os hamatum*, d4 in Fig. 5A) was partly or fully split in two distinct bones in about half of the double heterozygous mutants (Fig. 5C, arrow). A full separation of these bones, which originate as two separate fetal cartilages, was usually seen in *Hoxd-13*$^{-/-}$ specimens (not shown). Note, however, that metacarpal-phalangeal bone fusions occurred in *Hoxd-13*$^{-/-}$ mutants, but not in compound heterozygotes (Fig. 4B,D).

Altogether, the various limb alterations present in adult *Hoxa-13*$^{+/-}$/*Hoxd-13*$^{+/-}$ compound heterozygotes (summarized in Table 2) can be considered as: (1) a subset of the *Hoxd-13*$^{-/-}$ phenotypic traits, and (2) alterations which are reminiscent of the *Hoxa-13*$^{-/-}$ fetal phenotype and/or are observed in a milder form in *Hoxa-13*$^{+/-}$ heterozygous mutants and thus are probably related to the *Hoxa-13* haploinsufficiency.

Hoxa-13$^{+/-}$/*Hoxd-13*$^{-/-}$ compound mutants show a severe exacerbation of the *Hoxd-13*$^{-/-}$ phenotype together with novel limb abnormalities

Intercrosses between compound heterozygotes generated *Hoxa-13*$^{+/-}$/*Hoxd-13*$^{-/-}$ double mutants that were viable, but showed severe alterations of the forelimb (Fig. 6A) and hindlimb (Fig. 6D) autopods. There were no individual digits and the extremities of the forepaws consisted of a continuous ridge (Fig. 6A, arrowhead), whereas some claws were apparent at the hindpaw extremities (Fig. 6D, arrowhead). Skeletal preparations showed that the forelimb autopod skeleton was drastically truncated (Fig. 6B). The digits consisted of short metacarpal/phalangeal bones (‘M’; Fig. 6C) fused together to various extents, and terminal phalangeal-like structures fused to yield a common ‘terminal arch’ (‘TA’; Fig. 6B,C). The proximal carpal bones appeared normal [Fig. 6B,C; see the prepollex (pp) and pisiform (pi) bones], but the distal carpal bones were severely fused (Fig. 6B and data not shown). The hindlimb digits were also drastically truncated and deformed (Fig. 6E), and no individualized metatarsal and phalangeal bones could be seen. Terminal phalanges were visible in digits II-V, but were partly fused together (Fig. 6E, arrowhead). Note that the altered digit I of double mutants resembled the first metatarsal bone of single *Hoxd-13*$^{-/-}$ mutants (compare Fig. 6E with Fig. 4H). As in the forelimbs, the proximal tarsal bones were normal, but the distal tarsals were abnormally fused (Fig. 6E, and data not shown).

The chondrogenic patterns of *Hoxa-13*$^{+/-}$/*Hoxd-13*$^{-/-}$ mutant limbs were examined at various stages of development. We found that 13.5 dpc double mutant forelimbs consistently harbored a supernumerary digit cartilage condensation. However, a central condensation (often that of presumptive digit III) was fused distally to one of its neighbors (Fig. 7B, open arrow). Thus, only five digital swellings were apparent at the surface of the autopod (Fig. 7B). Abnormal cartilage connections also occurred between the presumptive digit IV and V condensations (Fig. 7B, arrowhead *). A small seventh posterior digit condensation was present in 14.5 dpc double mutant forelimbs (Fig. 7D; see also Fig. 8B). In most cases, the third digit cartilage was either prematurely truncated (Fig. 8B, *) or joined distally to the second cartilage (Fig. 7D, open arrow), and there were only six external digit swellings. Note, however, that none of the digits became properly separated. All digit cartilages were smaller than in WT littermates and showed almost no segmentation of metacarpal or phalangeal elements (Figs 7C,D and 8A,B). The hindlimbs of 14.5 dpc *Hoxa-13*$^{+/-}$/*Hoxd-13*$^{-/-}$ mutants were not polydactylous, but showed smaller and poorly segmented digit cartilages, as well as a lack of digit separation (Fig. 8E,F).

Examination of 18.5 dpc specimens confirmed these observations and revealed additional abnormalities. All *Hoxa-13*$^{+/-}$/*Hoxd-13*$^{-/-}$ forelimbs were polydactylous, with seven truncated and non-ossified digits (Fig. 7G,H). In about half of the cases, one of the central digits was prematurely fused to one or both of its neighbors (Fig. 7G, open arrow, and data not shown). The size of the digit cartilages decreased toward the anterior and posterior margins of the autopod and the entire forefoot had a symmetrical round shape (Fig. 7G,H). Since most of the double mutant digits were not segmented, it was impossible to assign to them a WT digit identity. In addition, there were more or less severe cartilaginous fusions between the distal extremities of the digits (Fig. 7G,H). Consequently, terminal ossification tended to proceed along a continuous ridge (Fig. 7H, dashes) rather than at the tip of each digit (Fig. 7E,F). Histological sections of 1 week-old newborns confirmed the presence of cartilaginous and bony fusions between the digit extremities and showed the presence of a continuous nail plate along the forefoot extremity (data not shown). The carpal cartilages were well developed and included an abnormally large central blastema and extra distal cartilages related to the presence of supernumerary digits (Fig. 7H, and data not shown).

Thus, the inactivation of a single *Hoxa-13* allele clearly had dramatic consequences for the developing forelimbs of *Hoxd-*

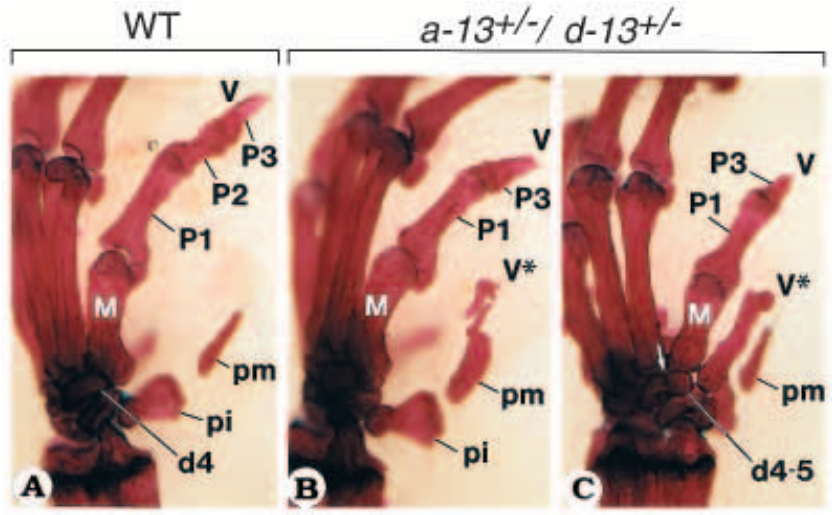

Fig. 5. Posterodorsal views of the forepaw skeleton of WT (A) and *Hoxa-13*$^{+/-}$*/Hoxd-13*$^{+/-}$ (B,C) adult mice, showing the abnormal digit V and the presence of a supernumerary digit rudiment (V*) in compound heterozygous mutants. The arrow in C shows a partial splitting of the *os hamatum* (distal carpal 4), which may result from the incomplete fusion of the two cartilages giving rise to this bone during development. d4, *os hamatum* (distal carpal 4); d4-5, *os hamatum* partly split in two separate bones; M, metacarpal bone; P1-P3, phalangeal bones; pi, pisiform; pm, post-minimus. Digits are numbered with roman numerals.

13$^{-/-}$ mutants (Fig. 7F-H). At 18.5 dpc, *Hoxd-13*$^{-/-}$ mutant forelimbs showed a lack of segmentation between certain metacarpal and first phalangeal cartilages (Fig. 7F, brackets), selective truncation and delay in the ossification of digits II and V, and a rudimentary posterior supernumerary digit cartilage (Fig. 7F, V*). In some aspects, the *Hoxa-13*$^{+/-}$*/Hoxd-13*$^{-/-}$ forelimb phenotype can be considered as an exacerbation of *Hoxd-13*$^{-/-}$ abnormalities (see Discussion), but terminal cartilage fusions were never seen in *Hoxd-13*$^{-/-}$ single mutants (Fig. 7F-H).

The 18.5 dpc *Hoxa-13*$^{+/-}$*/Hoxd-13*$^{-/-}$ mutant hindlimbs were not polydactylous. As observed in the forelimbs, the hindlimb digit cartilages were severely truncated and almost not segmented, but were not terminally fused (data not shown). Thus, the additional inactivation of one *Hoxa-13* allele in *Hoxd-13*$^{-/-}$ mutants increased the degree of truncation of hindlimb digits and generated defects of digit segmentation that were quasi-nonexistent in *Hoxd-13*$^{-/-}$ mutant hindlimbs (Dollé et al., 1993).

Hoxa-13$^{-/-}$*/Hoxd-13*$^{+/-}$ and *Hoxa-13*$^{+/-}$*/Hoxd-13*$^{-/-}$ mutants exhibit distinct limb phenotypes

Hoxa-13$^{-/-}$*/Hoxd-13*$^{+/-}$ double mutants could be recovered for analysis up to 14.5 dpc. These animals clearly displayed a more severe limb phenotype than *Hoxa-13*$^{-/-}$ single mutants (Fig. 8C,G). Nevertheless, this limb phenotype was clearly distinct from that of *Hoxa-13*$^{+/-}$*/*

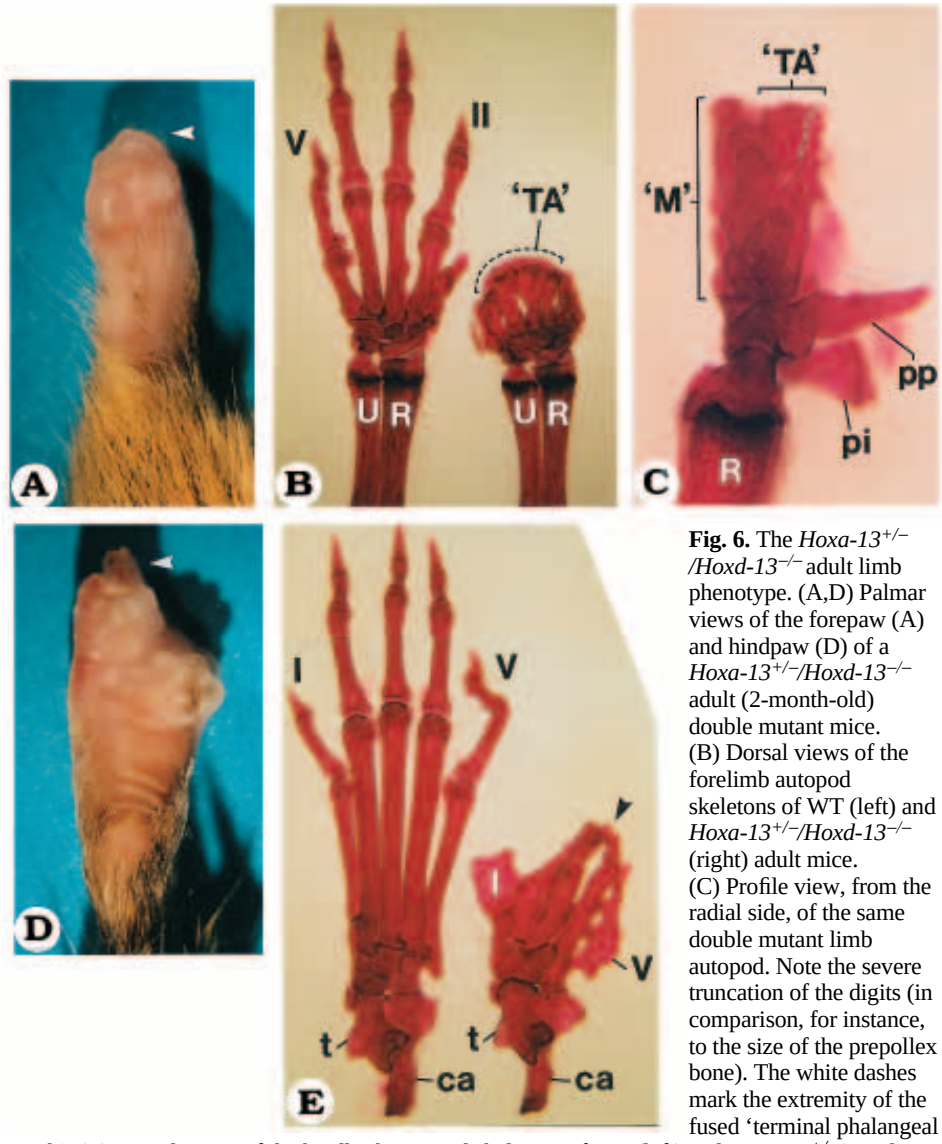

Fig. 6. The *Hoxa-13*$^{+/-}$*/Hoxd-13*$^{-/-}$ adult limb phenotype. (A,D) Palmar views of the forepaw (A) and hindpaw (D) of a *Hoxa-13*$^{+/-}$*/Hoxd-13*$^{-/-}$ adult (2-month-old) double mutant mice. (B) Dorsal views of the forelimb autopod skeletons of WT (left) and *Hoxa-13*$^{+/-}$*/Hoxd-13*$^{-/-}$ (right) adult mice. (C) Profile view, from the radial side, of the same double mutant limb autopod. Note the severe truncation of the digits (in comparison, for instance, to the size of the prepollex bone). The white dashes mark the extremity of the fused 'terminal phalangeal arch'. (E) Dorsal views of the hindlimb autopod skeletons of WT (left) and *Hoxa-13*$^{+/-}$*/Hoxd-13*$^{-/-}$ (right) adult mice. The arrowhead indicates a terminal fusion between digits II to IV. ca, calcaneus; 'M', truncated 'metacarpo-phalangeal' bones; pi, pisiform; pp, prepollex; R, radius; t, talus; 'TA', 'terminal phalangeal arch'; U, ulna. Digits are numbered with roman numerals.

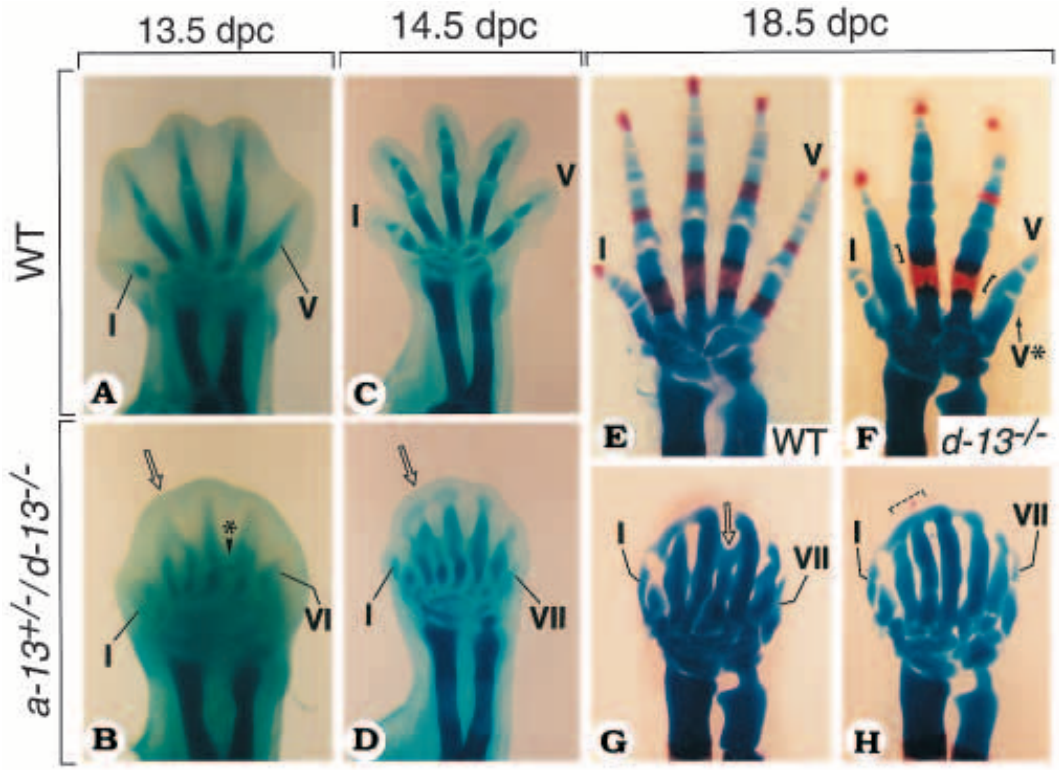

Fig. 7. Developmental alterations in *Hoxa-13*$^{+/-}$/*Hoxd-13*$^{-/-}$ double mutant forelimbs. (A,B) Dorsal views of the forelimb extremities from a 13.5 dpc WT and a double mutant fetus, respectively. The open arrow indicates the distal fusion between two digit cartilage condensations. The asterisk (*) indicates an abnormal link between digit condensations IV and V. Such connections were not seen in older fetuses, suggesting that they do not undergo sustained chondrification. (C,D) Dorsal views of the forelimb extremities from a 14.5 dpc WT and a double mutant fetus, respectively. The open arrow points to the distal fusion between two digit cartilages. (E-H) Dorsal views of a WT (E), *Hoxd-13*$^{-/-}$ (F) and two *Hoxa-13*$^{+/-}$/*Hoxd-13*$^{-/-}$ (G,H) forefeet skeletons at 18.5 dpc. The brackets in F show non- or poorly segmented metacarpo-phalangeal cartilages in the *Hoxd-13*$^{-/-}$ single mutant. The open arrow in G shows the fusion of a central digit cartilage to both of its neighbors. The dashes in H indicate a continuous rim of ossification along each side of a terminal ossification centre. Digits are numbered with roman numerals.

Hoxd-13$^{-/-}$ mutants at the same stage (Fig. 8B,C and F,G; Table 3). Although both genotypes resulted in a lack of digit separation, the external shape of the autopods was different: *Hoxa-13*$^{-/-}$/*Hoxd-13*$^{+/-}$ mutant footplates were narrower, especially toward their distal extremities (Fig. 8C,G). *Hoxa-13*$^{-/-}$/*Hoxd-13*$^{+/-}$ forelimbs displayed no digit I, no supernumerary central digit and a minute posterior supernumerary digit cartilage (Fig. 8C, V*). The lack of segmentation in the existing digits and a tendency toward the fusion of some terminal phalangeal condensations were reminiscent of the *Hoxa-13*$^{+/-}$/*Hoxd-13*$^{-/-}$ phenotype (Fig. 8B,C, arrows). With the exception of an altered pisiform cartilage, there was no individualization of carpal condensations in *Hoxa-13*$^{-/-}$/*Hoxd-13*$^{+/-}$ forelimbs (Fig. 8C), whereas most of the carpal elements were defined in *Hoxa-13*$^{+/-}$/*Hoxd-13*$^{-/-}$ mutants (Fig. 8B).

The hindlimbs of *Hoxa-13*$^{-/-}$/*Hoxd-13*$^{+/-}$ mutants harbored condensations for digits II to V, but these were irregular and remained in a primitive state. In particular, there was almost no chondrification in digit rays II and V (Fig. 8G). The entire tarsus was more altered than in *Hoxa-13*$^{+/-}$/*Hoxd-13*$^{-/-}$ mutants. Indeed, none of the tarsal blastemas was properly individualized and there was no separation line between the putative proximal and distal rows of the tarsus (Fig. 8F,G, white arrowheads).

Homozygous disruption of both *Hoxa-13* and *Hoxd-13* genes abolishes patterning of the limb autopod

The *in utero* lethality of *Hoxa-13*$^{-/-}$/*Hoxd-13*$^{-/-}$ double homozygous mutants was similar to that of *Hoxa-13*$^{-/-}$ mutants. However, the living double homozygous mutant fetuses were smaller than their littermates (data not shown). At 12.5-14.5 dpc, the limb autopods had a round shape with no

Table 3. Summary of the major abnormalities of the cartilage pattern in the forelimb autopodium of *Hoxa-13* and *Hoxd-13* single and compound mutant fetuses

	Mutant			
Limb abnormality	*Hoxa-13*$^{-/-}$ *Hoxd-13*$^{+/+}$	*Hoxa-13*$^{+/+}$ *Hoxd-13*$^{-/-}$	*Hoxa-13*$^{-/-}$ *Hoxd-13*$^{+/-}$	*Hoxa-13*$^{+/-}$ *Hoxd-13*$^{-/-}$
Lack of digit I	+	–	+	–
Lack of second phalanges (digits II and V)	+	+	+	+
Supernumerary posterior digit rudiment	–	+	(+)	+
Supernumerary central digits	–	–	–	+
Altered digit segmentation	–	(+)	+	+
Fusions between terminal phalanges	–	–	(+)	+
Altered carpal morphogenesis	+	–	+	+

External morphological alterations of the autopodium are not recorded here (see Results and Figs 1, 2 and 6).

+, fully penetrant abnormality; (+), incompletely penetrant or milder abnormality; –, no abnormality.

external sign of digit formation and were more truncated than those of any other mutant genotype (Fig. 8D,H, and data not shown; see also Fig. 9A). Although smaller in size, the *Hoxa-13*$^{-/-}$/*Hoxd-13*$^{-/-}$ limbs exhibited a normal pattern of chondrification and ossification down to the extremities of the radius/ulna and tibia/fibula (Fig. 9B, and data not shown). In contrast, there was almost no patterning of preskeletal elements distal to these extremities. At 14.5 dpc, the chondrogenic activity was diffuse in the entire central core of the hindlimb autopod (Fig. 8H), whereas, in the forelimbs, it was increased along two ill-defined areas extending distally from the radius and ulna cartilages (Fig. 8D).

The oldest double homozygous mutant was obtained from a litter of four pups that were prematurely delivered at 16.5-17.5 dpc. This specimen displayed severely truncated limb autopods (Fig. 9B-D). As observed at 14.5 dpc, chondrogenic cells were distributed in the entire central core of the forelimb (Fig. 9B,C) or hindlimb (Fig. 9D) autopods. At the forelimb level, chondrogenesis was enhanced along a single posterior condensation in continuity with the ulna (Fig. 9C, arrow), and some putative carpal condensations were located distally to the radius (Fig. 9C). There were no visible digital arch or primary digit condensations. In the hindlimb, a cartilage connection existed between the fibula and the autopod central core (Fig. 9D). Except for a proximal condensation, which may correspond to the calcaneus primordium, there was no other sign of preskeletal pattern in the hindlimb autopod (Fig. 9D).

DISCUSSION

Hoxa-13 function in developing limbs

The development of the tetrapod limb can be described as a series of condensation, branching and segmentation events. The main axis of condensation (the metapterygian axis) runs along the humerus (stylopod), the ulna and the ulnare (zeugopod), and then bends anteriorly through the autopod, thus forming a digital arch from which each distal carpal (tarsal) and metacarpal (metatarsal) condensation will successively branch out (Shubin and Alberch, 1986). In dipnoan fishes, there is no bending of the metapterygian axis, leading to the fish fin, which would correspond to a truncated limb without autopod (Sordino et al., 1995). We show here that the *Hoxa-13*$^{-/-}$ limb phenotype differs from that of *Hoxd-13*$^{-/-}$ mutants (Dollé et al., 1993) both in terms of spatial distribution and in the nature of the abnormalities. The *Hoxd-13*$^{-/-}$ mutation specifically affects the development of postaxial structures of the autopod (derived from branching events on the posterior side the 'metapterygial axis'), i.e. there is reduction in size, particularly of digit I, II and V, or loss of phalanges, fusion of carpal and tarsal elements and occasional production of a supernumerary sixth digit. On the contrary, the *Hoxa-13*$^{-/-}$ mutation affects structures that derive both from postaxial and preaxial branching events: the most severely affected carpal elements (the scapholunatum and central bone anlagen) derive from the centrale and intermedium cartilages, which arise through preaxial branching from the ulnare (Shubin and Alberch, 1986). Interestingly, the radius and ulna cartilages are not altered, in keeping with the observation that *Hoxa-13* is not expressed in the developing zeugopodal elements (Haack and Gruss, 1993; and our unpublished data). The branching of all five digits occurs in *Hoxd-13*$^{-/-}$ mutants, but their subsequent growth and chondrification pattern are affected (Dollé et al., 1993). On the contrary, the *Hoxa-13*$^{-/-}$ mutants lack the most anterior digit (digit I) in both forelimbs and hindlimbs, except for a minute condensation seen in 15.5 dpc mutant forelimbs. In addition, the most posterior digit (digit V) of the hindlimb remains in the state of a small precartilaginous condensation.

Thus, it appears that the *Hoxa-13*$^{-/-}$ mutant limb phenotype shows no evidence of homeotic transformation, but displays features of heterochrony that are more pronounced than in the case of the *Hoxd-13*$^{-/-}$ mutation (Dollé et al., 1993). The *Hoxa-13*$^{-/-}$ limb phenotype may result from a retardation or an arrest in the sequence of pattern formation in the autopod. The digits that develop poorly or not at all in *Hoxa-13*$^{-/-}$ mutants are the last ones to appear during development of non-urodele tetrapods (Müller, 1991). Interestingly, there are natural examples of digit number reduction in lizards. Lizards of a single genus (*Lerista*) can exhibit a wide range of digit reduction but digits I, or I and V, are the first two digits that are missing in animals lacking one or two digits, respectively (Greer, 1990). Reduction of digit number can also be generated experimentally by applying the mitotic inhibitor ara-C to the limb mesenchyme of *Lacerta* lizards (Raynaud and Clergue-Gazeau, 1986). In these experiments, digit I was also the first to be lost. The *Hoxa-13*$^{-/-}$ mutation is the first example of a targeted *Hox* mutation that generates a selective lack of digits, and thus mimicks a natural evolutionary trend observed in certain species.

The carpal and tarsal alterations in *Hoxa-13*$^{-/-}$ mutants also correlate with the temporal sequence of ontogenic development. Indeed, the pisiform, pyramidal (*triquetrum*) and distal carpal 4 (*hamatum*), whose development is less affected by the *Hoxa-13*$^{-/-}$ loss-of-function, are known to develop earlier and faster than the other carpal elements and, therefore, are part of the amniote limb 'primary axis' defined by Burke and Alberch (1985). On the contrary, the carpal preaxial elements that are not discernable in *Hoxa-13*$^{-/-}$ mutants are those which develop last in the ontogenic sequence. Similar conclusions can be drawn in the case of the hindlimb, since the posterior tarsal blastemas are less affected than the anterior ones in *Hoxa-13*$^{-/-}$ mutants. Thus, *Hoxa-13*$^{-/-}$ mutants display features reminiscent of a delay in the development of the digit primary condensations and carpal (tarsal) blastemas, which are the last to appear during ontogenesis. Unfortunately, due to the fetal lethality of *Hoxa-13* null mutants, it is unknown whether this delay might lead to the generation of neotenic limbs.

Yokouchi et al. (1995) have reported that ectopic expression of *Hoxa-13* in chick limb buds selectively affects zeugopodal cartilages, conferring on them some features of carpal/tarsal cartilages. These observations are consistent with the fact that the targeted disruption of *Hoxa-13* affects the development of some carpal and tarsal cartilages. In addition, misexpression of *Hoxa-13* sometimes generates a supernumerary anterior digit cartilage in both wing and leg (Yokouchi et al., 1995). Thus, *Hoxa-13* misexpression and loss-of-function studies indicate a prominent role of this gene in the generation of carpal/tarsal elements and in the control of digit formation. Our results, however, provide no support for a model where *Hoxa-13* would be involved in the production of a repressive signal leading to growth arrest of carpal and tarsal cartilages, in order

to allow them to develop as short bones (Yokouchi et al., 1995). Indeed, the present *Hoxa-13* loss of function did not result in an excessive development of carpal and tarsal cartilages, at least up to 15.5 dpc. Yokouchi et al. (1995) also proposed that *Hoxa-13* may be involved in determining homophilic cell-to-cell adhesiveness properties since (1) ectopic expression of *Hoxa-13* results in the formation of ectopic precartilaginous condensations, and (2) in limb bud mesenchymal cell cultures, *Hoxa-13*-expressing cells are able to selectively reassociate and form aggregates. Accordingly, *Hoxa-13* would play a role in the segmentation and bifurcation of precartilaginous condensations through control of local cell-to-cell adhesiveness properties. This proposal is consistent with the observation that *Hoxa-13* inactivation apparently disrupts certain branching events leading to the lack of, for example, digit I and the scapholunate cartilages. Alternatively, the *Hoxa-13* phenotype may result from mesenchymal cell deficiency in the autopod due to decreased growth rates, or to an extension of the area of programmed cell death in the mesenchyme underlying the AER (Milaire, 1967). Extended areas of mesenchymal cell death are believed to be the basis for the absence of digit I in some species, especially in the case of the chick wing bud (Hinchliffe and Johnson, 1980). We are currently investigating the patterns of cell proliferation and cell death in *Hoxa-13*$^{-/-}$limb buds.

Polydactyly in *Hoxa-13*$^{+/-}$*/Hoxd-13*$^{-/-}$ mutants

Hoxa-13$^{+/-}$*/Hoxd-13*$^{-/-}$ compound mutants were viable, but displayed more severe abnormalities than single *Hoxd-13*$^{-/-}$ mutants. Their forelimbs were polydactylous: seven digit cartilages appeared, remained much shorter than in WT and *Hoxd-13*$^{-/-}$ specimens, and did not undergo proper segmentation of the metacarpal and phalangeal cartilages. Digit size symmetrically decreased toward the anterior and posterior sides of the footplate. In addition, cartilaginous and bony fusions developed between the extremities of most digits. Thus, none of the double mutant digits were morphologically similar to WT or *Hoxd-13*$^{-/-}$ digits. In contrast, there was no polydactyly in the hindlimbs, and the digits, although severely truncated, still bear some resemblance to those of *Hoxd-13*$^{-/-}$ hindlimbs. However, as in the case of the forelimb, most metatarsal and phalangeal cartilages were non-segmented and there were limited fusions between some digit extremities.

Whereas numerous tetrapod lineages display a reduced digit number with respect to the pentadactyl archetype, there has never been an evolutionary trend toward the acquisition of supernumerary digits, and polydactyly only occurred in some laboratory mutant strains. The final digit number, in a given species, seems to be related to the anteroposterior length (or the ratio between anteroposterior and dorsoventral length) of the limb bud autopod (Hinchliffe and Johnson, 1980, and refs therein). However, *Hoxa-13*$^{+/-}$*/Hoxd-13*$^{-/-}$ mutant fetuses displayed two supernumerary forelimb digit cartilage condensations, despite the fact that the autopods were not exaggerately enlarged anteroposteriorly. The spacing between digit condensations was reduced and, in most instances, one of the central digit condensations did not reach the autopod extremity, but became fused to one of its neighbors as early as 13.5 dpc. Older fetuses consistently had one of their central digit cartilages prematurely aborted or fused to its neighbor(s). These defects clearly suggest that the double mutant genotype results in abnormal branching of two supernumerary digit condensations in an autopod whose anteroposterior length is not sufficient to accommodate all the supernumerary digits. Interestingly, the mouse mutant shaker with syndactylism (*sy*) is not polydactylous, but shows similar distal fusion between two hindlimb digit cartilages. In that case, fusion appears to be related to a reduction in size of the 12.5 dpc mutant autopod (Grüneberg, 1962).

Can the polydactyly of *Hoxa-13*$^{+/-}$*/Hoxd-13*$^{-/-}$ mutants be considered an atavism? Devonian fossil digited stem tetrapods (*Acanthostega* and *Ichtyostega*) were polydactylous (Coates and Clack, 1990; Coates, 1991). Their limbs harbored seven to eight polyphalangeal digits, including three serial shorter digits at the anterior side, which may have been lost during evolution to give rise to modern pentadactyl limbs. The polydactylous forelimbs of our genetically engineered mice consist of serial and symmetrically arranged digits that have no specific metacarpo/phalangeal pattern and, therefore, cannot be homologized to the digits of *Acanthostega* and *Ichtyostega*. Nevertheless, it is interesting that disruption of three out of the four *Hoxa-13/Hoxd-13* alleles leads to a polydactyly reminiscent of the earliest tetrapods, together with a loss of digit 'identities'. However, it cannot be excluded that the insertion of the Neomycine selection cassette and thus the presence of an additional promoter in the *Hox* cluster could result in *Hox* gene ectopic expression, and therefore be the cause of some of the present abnormalities, including polydactyly. Indeed, such selection cassette insertions may disrupt the expression of the neighbor genes and therefore confound the interpretation of the phenotypes (Olson et al., 1996).

Dosage effects and functional redundancy among *Hox* genes in the developing autopod

While both *Hoxa-13*$^{+/-}$ and *Hoxd-13*$^{+/-}$ heterozygous mutants showed minor limb alterations, compound heterozygous mutants displayed a markedly altered phenotype, reproducing some of the abnormalities generated either by *Hoxa-13* or *Hoxd-13* loss of function (see Table 2). The truncation or lack of second phalangeal bones in digits II and V of both limbs, and the presence of a rudimentary posterior sixth digit in the forelimbs, was reminiscent of the *Hoxd-13*$^{-/-}$ phenotype. On the contrary, both forelimb and hindlimb first digit alterations were distinct from those of *Hoxd-13*$^{-/-}$ mutants, but were found, in a milder form, in single *Hoxa-13*$^{+/-}$ heterozygotes. The interdigital soft tissue fusions of compound heterozygotes also have a milder counterpart in *Hoxa-13*$^{+/-}$ heterozygotes, and are reminiscent of the poor digit separation seen in *Hoxa-13*$^{-/-}$ fetuses.

Previously described examples of such non-allelic non-complementation in yeast or *Drosophila* often involve genes whose products interact in oligomeric combinations (e.g. Rine and Herskowitz, 1987; Stearns and Botstein, 1988; Hays et al., 1989). Although interactions between certain Hox proteins have been documented (Zappavigna et al., 1994), there is no evidence to date that the Hoxa-13 and Hoxd-13 gene products may function as heterodimers. However, their homeodomain sequence similarities suggest that both proteins may have similar binding specificities and, thus, share a partly overlapping repertoire of target binding sites. This could explain why some phenotypic effects are 'quantitative', i.e. are generated by the reduction in the amount of Hoxa-13 and/or Hoxd-13

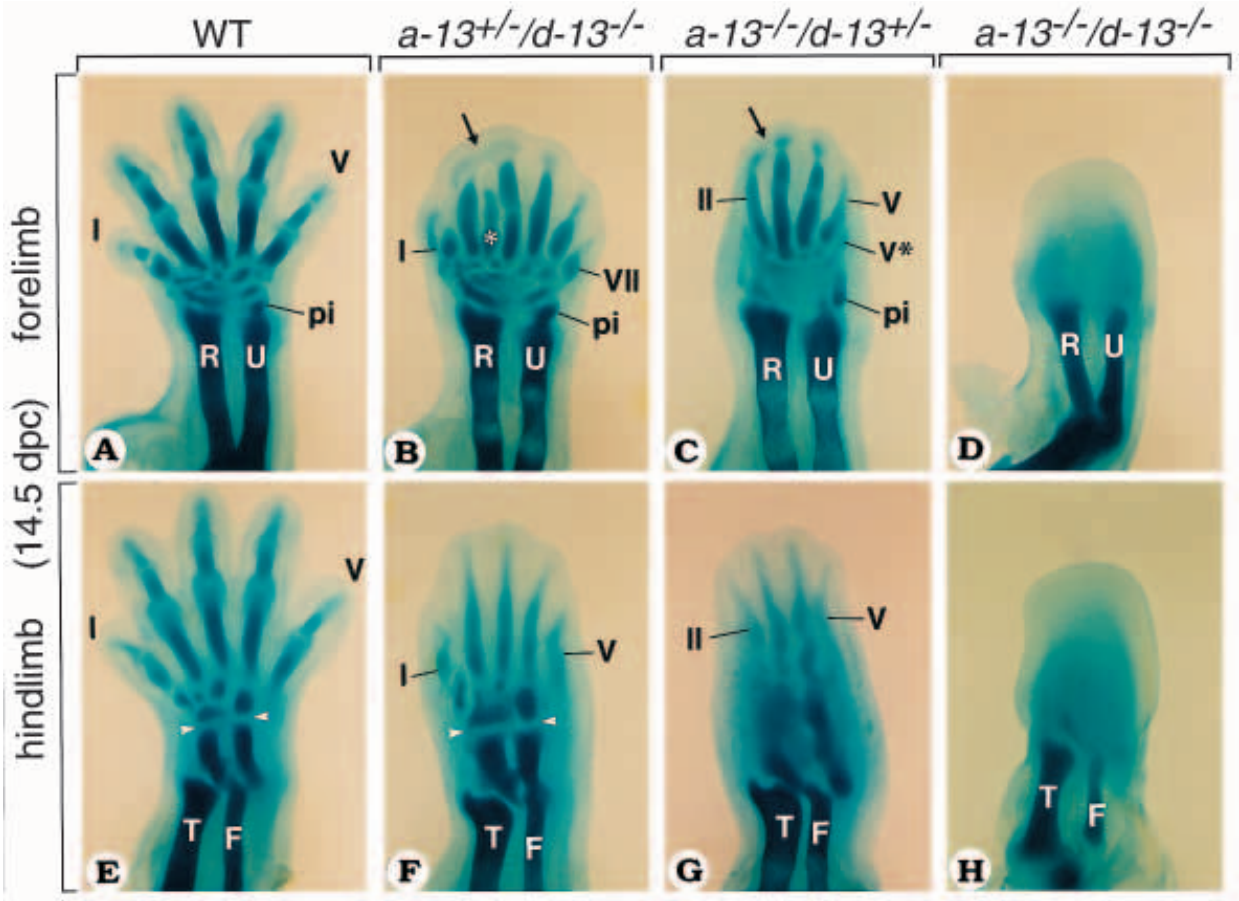

Fig. 8. Comparison of the forelimb (A-D) and hindlimb (E-H) phenotypes of WT (A,E), *Hoxa-13*$^{+/-}$*/Hoxd-13*$^{-/-}$ (B,F), *Hoxa-13*$^{-/-}$*/Hoxd-13*$^{+/-}$ (C,G) and *Hoxa-13*$^{-/-}$*/Hoxd-13*$^{-/-}$ (D,H) compound mutant fetuses at 14.5 dpc. The asterisk in B indicates an aborted digit condensation. Thus, although seven digit condensations have arisen proximally, only six of them reached the extremity of the autopod and produced digital swellings. The arrows in B and C show the tendency toward a fusion between adjacent terminal phalangeal cartilages. The white arrowheads in E and F point to the separation line between proximal and distal tarsal cartilages, which is well-defined in *Hoxa-13*$^{+/-}$*/Hoxd-13*$^{-/-}$, but not in *Hoxa-13*$^{-/-}$*/Hoxd-13*$^{+/-}$ mutants (G). F, fibula; pi, putative pisiform condensation; R, radius; T, tibia; U, ulna. Digits are numbered with roman numerals.

gene products below a critical threshold, irrespective of the type of protein remaining.

Non-allelic non-complementation was also observed, to a lesser extent, between *Hoxa-11* and *Hoxd-11*, since double heterozygous mutants displayed some of the carpal abnormalities seen in both *Hoxa-11*$^{-/-}$ and *Hoxd-11*$^{-/-}$ mutants (Davis et al., 1995). In this study, mutants harboring a single WT allele of either *Hoxa-11* or *Hoxd-11* had indistinguishable phenotypes consisting of a marked truncation of the radius and ulna. We analyzed mice with a single remaining functional allele of either *Hoxa-13* or *Hoxd-13* up to 14.5 dpc, and found that each genotypic combination produced a distinct limb phenotype. The three major differences were: (1) distinct alterations of the shape of the autopods, those of *Hoxa-13*$^{-/-}$*/Hoxd-13*$^{+/-}$ mutants being narrower along the anteroposterior axis; (2) distinct digit formulae; *Hoxa-13*$^{-/-}$*/Hoxd-13*$^{+/-}$ mutants display a lack of digit I in both limbs and a minute supernumerary posterior digit cartilage in the forelimbs, as well as very rudimentary hindlimb digit condensations, whereas *Hoxa-13*$^{+/-}$*/Hoxd-13*$^{-/-}$mutants exhibit a polydactyly with seven digits at the level of the forelimb; (3) distinct carpal and tarsal phenotypes, with more severe alterations in *Hoxa-13*$^{-/-}$*/Hoxd-13*$^{+/-}$ mutants. However, some phenotypic alterations, such as the poor segmentation of metacarpal (metatarsal)/phalangeal cartilages or the persistent absence of digit separation, were common to both double mutant genotypes. We conclude that, in contrast to *Hoxa-11* and *Hoxd-11* in the developing zeugopod, single remaining non-disrupted *Hoxa-13* or *Hoxd-13* alleles are not functionally equivalent for autopodal development.

Whereas the quantitative reduction of gene product generated by each individual heterozygous mutation is sufficient to allow an almost normal development, the combined reduction of both gene products in compound heterozygotes leads to marked phenotypic alterations. Interestingly, only part of the alterations seen in *Hoxa-13*$^{-/-}$ or *Hoxd-13*$^{-/-}$ mutants are observed in compound heterozygotes (Table 2). Thus, some of the alterations seen in *Hoxa-13*$^{-/-}$ and *Hoxd-13*$^{-/-}$ mutants correspond to quantitative rather than qualitative effects, i.e. can result from a reduction in the total amount of Hoxa-13 and Hoxd-13 gene products, irrespective of the type of protein lacking, whereas the generation of other alterations depend on the elimination of either the Hoxa-13 or the Hoxd-13 protein.

These double heterozygote results, as well as the abnormalities observed with the other double mutants, also indicate that

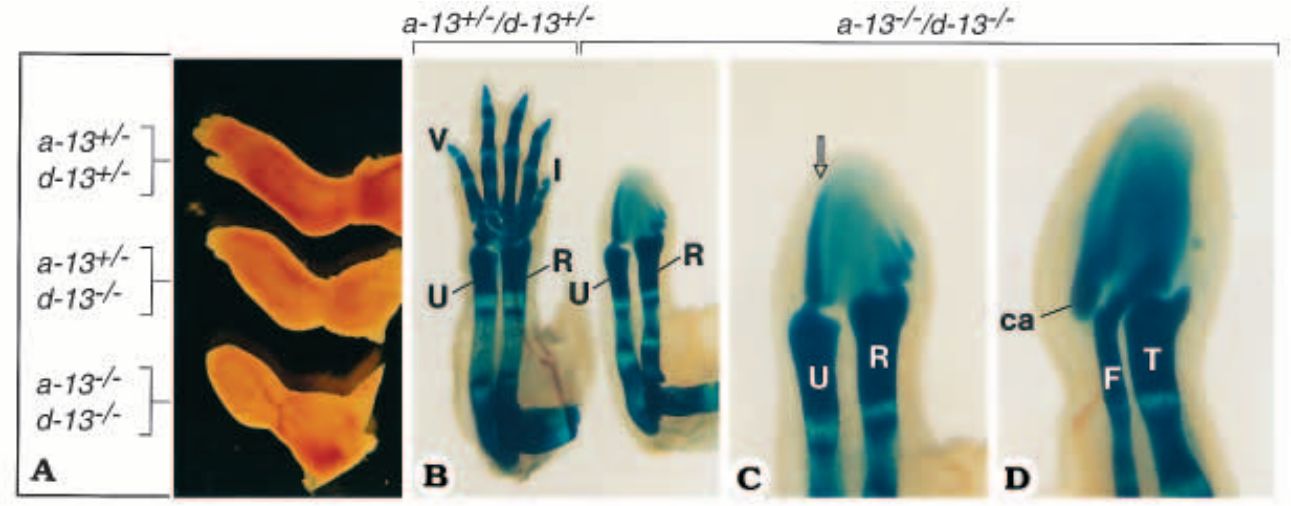

Fig. 9. The *Hoxa-13*$^{-/-}$*/Hoxd-13*$^{-/-}$ limb phenotype. (A) Comparison of the external morphology of the forelimb extremities of three littermate 16.5 dpc fetuses with increasing numbers of disrupted *Hoxa-13* and *Hoxd-13* alleles (as indicated). (B) Cartilaginous patterns of the forelimbs of a 16.5 dpc *Hoxa-13*$^{-/-}$*/Hoxd-13*$^{-/-}$ double homozygous mutant and a 'control' (*Hoxa-13*$^{+/-}$*/Hoxd-13*$^{+/-}$) littermate. In addition to the autopod phenotype, note that the radius and ulna of the double homozygous mutant are reduced in size, but have a normal morphology and ossification status. (C) High magnification view of the forelimb autopod from the double homozygous mutant shown in B. The open arrow shows the single posterior cartilage condensation. (D) High magnification view of the hindlimb autopod from the same animal. ca, putative calcaneus condensation; F, fibula; R, radius; T, tibia; U, ulna. Digits are numbered with roman numerals.

the Hoxa-13 and Hoxd-13 gene products act in a partly redundant manner in the developing limbs. Indeed, the phenotype of each compound mutant is more severe than the sum of the phenotypes observed for the corresponding single mutants. Recent studies have shown that the *Hoxd-13*, *d-12* and *d-11* genes act in a partly redundant manner in the developing forelimb autopod. Indeed, various trans-heterozygous compound mutants displayed specific abnormalities that are also seen in one (or both) of the corresponding homozygous mutants (Davis and Capecchi, 1996; see also Kondo et al., 1996). From these and the present results, it clearly appears that a fine balance between various Hoxa and Hoxd gene products is required for proper growth and patterning of (at least the forelimb) autopodal skeletal elements.

Hoxa-13 and *Hoxd-13* are essential for patterning of the autopod

Hoxa-13 and *Hoxd-13* have an additional paralogue, *Hoxc-13*, which is apparently not expressed in the developing limbs (Peterson et al., 1994). Thus, compound homozygous disruptions of both *Hoxa-13* and *Hoxd-13* should result in the complete lack of gene products from the homology group 13 in the developing autopods. We show here that this double loss of function results in severe alterations of growth and patterning of the autopods. Externally, both the forelimb and hindlimb autopods of double homozygous mutants were severely reduced in size and had a round shape with no apparent digits. Furthermore, there was almost no sign of chondrogenic patterning in the entire autopods of these mutants. At 14.5 dpc, chondrogenic cells were organized in a large central mass within each limb autopod, with two ill-defined cell aggregates extending beyond the radius and ulna cartilages in the forelimb. Thus, it appeared that the development of the autopods remained at a stage corresponding to the central chondrogenic blastemas characteristic of early developmental stages. In the oldest specimen analyzed, a condensed ray extended from the ulna extremity along the posterior margin of the central blastema. There was no equivalent discrete ray in the hindlimb, but a continuous condensation linked the fibula to the autopod central blastema. These posterior condensations may represent a rudimentary 'primary axis' of the autopod. This suggests that the lack of patterning in double homozygous mutant autopods may correspond to a premature truncation of the limb 'metapterygial axis' at the point where it bifurcates from a proximodistal to a posterior-anterior direction to form the digital arch, thereby precluding any further branching of postaxial condensations (digit anlagen). The bending of the metapterygial axis in the tetrapod lineage has been proposed to be a consequence of increased posterodistal cell proliferation during the terminal phase of limb growth, leading to an enlarged autopod (Duboule, 1994; Coates, 1995). It is tempting to speculate that the combined inactivation of *Hoxa-13* and *Hoxd-13*, which are expressed in the posterodistal region of early limb buds, may reduce the growth rate in the presumptive autopod region leading to premature truncation of the metapterygial axis, and thus to a structure resembling the fish fin, which appears like a truncated limb without autopod (Sordino et al., 1995). Alternatively, the sequential branching of digit condensations might be disrupted due to the loss of homophilic cell adhesion properties in the autopod mesenchyme, as discussed above.

Both mouse and human inherited limb abnormalities have been very recently correlated with group 13 *Hox* gene mutations. The human synpolydactyly (SPD) phenotype was shown to result from in-frame insertions of short poly(alanine) stretches in the aminoterminal region of the Hoxd-13 protein (Muragaki et al., 1996). Heterozygous patients exhibit a supernumerary central digit and syndactyly between digits III and IV, whereas homozygous mutant limbs present a shortening of the entire autopod with syndactyly between digits III, IV and

V. The mouse *Hypodactyly* (*Hd*) mutation (Hummel, 1970) has been genetically related to a deletion of 50 nucleotides in the first exon of the *Hoxa-13* gene, introducing a frameshift at the level of the aminoterminal part of the Hoxa-13 protein which, however, does not exclude the possible synthesis of a protein truncated at the N terminus and containing the homeobox (Mortlock et al., 1996). *Hd* is a semi-dominant lethal mutation, in which digits are shortened or deleted. The homozygous mutants, which seldom survive, harbor a single digit in each limb. The heterozygotes are viable and less severely affected, with only a shortening of all the four digits I. Both SPD and *Hd* have been proposed to be dominant negative mutations. Indeed, the limb abnormalities generated by both of these inherited conditions are more severe than those obtained by targeted inactivation of the corresponding genes through disruptions of their homeobox sequences (Dollé et al., 1993; this study). In this respect, we note that the SPD and *Hd* phenotypes mimick some of the abnormalities observed in *Hoxa-13/Hoxd-13* compound mutants. The polydactyly and syndactyly of SPD mutants resemble the *Hoxa-13*$^{+/-}$*/Hoxd-13*$^{-/-}$ or *Hoxa-13*$^{+/-}$*/Hoxd-13*$^{+/-}$ phenotypes, while the reduction of the autopod and presence of a single digit in *Hd/Hd* mice is to some extent comparable to the *Hoxa-13*$^{-/-}$*/Hoxd-13*$^{-/-}$ phenotype. These observations further support the possible existence of functional interactions between the Hoxa-13 and Hoxd-13 proteins, perhaps as heterodimeric partners (see above). Since both SPD and Hd mutations affect the aminoterminal region of the respective Hox proteins in a region rich in alanine residues, it appears that these N-terminal regions may correspond to functional domains necessary for these cooperative interactions.

In summary, three major conclusions can be drawn from our present study: (1) both *Hoxa-13* and *Hoxd-13* genes are indispensable for growth and patterning of the entire 'terminal' region of the developing limb (the autopod); (2) the products of the two genes are partially functionally redundant, however, since the phenotype of any double mutant is much more severe than the sum of the phenotypes seen in the corresponding single mutants; (3) the function of these two group 13 genes cannot be complemented by Hox genes belonging to paralogous groups located more 3′, although some of these genes are co-expressed in the developing autopod. Previous studies have shown that combined disruption of *Hoxa-11 and Hoxd-11* leads to severe size reduction of the forelimb zeugopodal elements (Davis et al., 1995). In contrast, double homozygous disruption of *Hoxa-9* and *Hoxd-9* results in mild reduction and morphological alteration of the stylopodal element (the humerus; Fromental-Ramain et al., 1996). Clearly, the phenotypic alterations generated by compound loss of functions of paralogous *Hox* genes are more drastic toward distal limb regions (i.e. for paralogues located 5′). Accordingly, the consequences of single *Hox* gene disruptions also seem to be more severe in distal regions, ranging from no detectable effect in the stylopod (e.g. in the case of *Hoxa-9*) to marked alterations in the autopod (in the cases of *Hoxa-13* and *Hoxd-13*). Altogether, it appears that the deleterious effects of individual or compound *Hox* mutations increase toward distal regions of the developing limbs, culminating in the autopod where patterning is strictly dependent on the activity of the Hoxa-13 and/or Hoxd-13 gene products. That the autopod is the limb segment which is the most sensitive to quantitative or qualitative changes in Hox protein combinations may provide a genetic basis to account for the evolutionary diversity of limb extremities in tetrapod lineages, which contrasts with the relative 'stability' of proximal limb structures.

We thank Professor P. Gruss and Dr Haack for their generous gift of *Hoxa-13* genomic DNA, Dr P. Simpson for a critical reading of the manuscript, C. Birling for excellent technical assistance all along this study, Dr A. Dierich, M. Diegelman and E. Blondelle for ES cell culture, V. Fraulob and B. Schuhbaur for technical assistance, and the technicians of the animal facilities. This work was supported by funds from the Institut National de la Santé et de la Recherche Médicale, the Centre National de la Recherche Scientifique, the Centre Hospitalier Universitaire Régional, the Association pour la Recherche sur le Cancer (ARC), the Fondation pour la Recherche Médicale (FRM) and the Ligue Nationale contre le Cancer.

REFERENCES

Archer, C.W., Cottril, C. and Rooney, P. (1984). Cellular aspects of cartilage differentiation and morphogenesis. In *Matrices and Differentiation* (ed R. Kemp and J.R. Hinchcliffe), pp. 305-322. New York: A. R. Liss.

Burke, A.C. and Alberch, **P.** (1985). The development and homologies of the chelonian carpus and tarsus. *J. Morphology* **186**, 119-131.

Coates, M.I. (1991). New paleontological contributions to limb ontogeny and phylogeny. In *Developmental Patterning of the Vertebrate Limb* (ed. J.R. Hinchliffe, J.M. Hurle, D. Summerbell), pp. 347-354. New York: Plenum.

Coates, M.I. (1995). Fish fins or tetrapod limbs - a simple twist of fate? *Current Biol.* **5**, 844-848.

Coates, M.I. and Clack, J.A. (1990). Polydactyly in the earliest known tetrapod limbs. *Nature* **347**, 66-68.

Crossley, P.H., Minowada, G., MacArthur, C.A. and Martin, G.R. (1996). Roles for FGF8 in the induction, initiation, and maintenance of chick limb development. *Cell* **84**, 127-136.

Davis, A.P. and Capecchi, M.R. (1994). Axial homeosis and appendicular skeleton defects in mice with a targeted disruption of *Hoxd-11*. *Development* **120**, 2187-2198.

Davis, A.P., Witte, D.P., Hsieh-Li, H.M., Potter, S.S. and Capecchi, M.R. (1995). Absence of radius and ulna in mice lacking *Hoxa-11* and *Hoxd-11*. *Nature* **375**, 791-795.

Davis, A.P. and Capecchi, M.R. (1996). A mutational analysis of the 5' HoxD genes: dissection of genetic interactions during limb development in the mouse. *Development* **122**, 1175-1185.

Dollé, P. and Duboule, D. (1993). Structural functional aspects of mammalian Hox genes. *Adv. Dev. Biochem.* **2**, 55-106.

Dollé, P., Dierich, A., LeMeur, M., Schimmang, T., Schuhbaur, B., Chambon, P. and Duboule, D. (1993). Disruption of the Hoxd-13 gene induces localized heterochrony leading to mice with neotenic limbs. *Cell* **75**, 431-441.

Dollé, P., Izpisua-Belmonte, J.C., Falkenstein, H., Renucci, A. and Duboule, D. (1989). Coordinate expression of the murine Hox-5 complex homeobox-containing genes during limb pattern formation. *Nature* **342**, 767-772.

Duboule, D. and Dollé, P. (1989). The structural and functional organization of the murine HOX gene family resembles that of Drosophila homeotic genes. *EMBO J.* **8**, 1497-1505.

Duboule, D. (1994). How to make a limb. *Science* **266**, 575-576.

Favier, B., Lemeur, M., Chambon, P. and Dollé, P. (1995). Axial skeleton homeosis and forelimb malformations in Hoxd-11 mutant mice. *Proc. Natl. Acad. Sci. USA* **92**, 310-314.

Favier, B., Rijli F.M., Fromental-Ramain C., Fraulob V., Chambon P. and Dollé, P. (1996). Functional cooperation between the non-paralogous genes *Hoxa-10* and *Hoxd-11* in the developing forelimb and axial skeleton. *Development* **122**, 449-460.

Francis, P.H., Richardson, M.K., Brickell, P.M. and Tickle, C. (1994). Bone morphogenetic proteins and a signalling pathway that controls patterning in the developing chick limb. *Development* **120**, 209-218.

Fromental-Ramain, C., Warot, X., Lakkaraju, S., Favier, B., Haack, H., Birling, C., Dierich, A., Dollé, P. and Chambon, P. (1996). Specific and redundant functions of the paralogous *Hoxa-9* and *Hoxd-9* genes in forelimb and axial skeleton patterning. *Development* **122**, 461-472.

Gossler, A., Doetschman, T., Korn, R., Serfling, E. and Kemler, R. (1986). Transgenesis by means of blastocyst-derived embryonic stem cell lines. *Proc. Natl. Acad. Sci. USA* **83**, 9065-9069.

Graham, A., Papalopulu, N. and Krumlauf, R. (1989). The murine and Drosophila homeobox gene complexes have common features of organization and expression. *Cell* **57**, 367-378.

Greer, A.E. (1990). Limb reduction in the Scincid lizard genus, Lerista. 2. Variations in the bone complements of the front and rear limbs and the number of post-sacral vertebrae. *J. Herpetol.* **24**, 142-150.

Grüneberg, H. (1962). Genetical studies on the skeleton of the mouse. XXV. The development of shaker with syndactylism. *Genet. Res. Camb.* **3**, 157-166.

Haack, H. and Gruss, P. (1993). The establishment of murine Hox-1 expression domains during patterning of the limb. *Dev. Biol.* **157**, 410-422.

Hays, T.S., Duering, R., Robertson, B., Prout, M. and Fuller, M.T. (1989). Interacting proteins identified by genetic interactions: A missense mutation in α-tubulin fails to complement alleles of the testis-specific β-tubulin gene of Drosophila melanogaster. *Mol. Cell. Biol.* **9**, 875-884.

Hinchiffe, J.R. and Johnson, D.R. (1980). *The Development of the Vertebrate Limb*. Oxford, UK: Oxford University Press.

Hummel, K. P. (1970). Hypodactyly, a semidominant lethal mutation in mice. *J. Hered*. **61**, 219-220.

Jegalian, B.G. and De Robertis, E.M. (1992). Homeotic transformation in the mouse induced by overexpression of a human Hox-3.3 transgene. *Cell* **71**, 901-910.

Kondo, T., Dollé, P., Zakany, J. and Duboule, D. (1996). Function of posterior HoxD genes in the morphogenesis of the anal sphincter. *Development*, in press.

McCarrick III, J.W., Parnes, J.R., Seong, R.H., Solter, D. and Knowles, B.B. (1993). Positive-negative selection gene targeting with the diphtheria toxin A-chain gene in mouse embryonic stem cells. *Transgenic Res*. **2**, 183-190.

McGinnis, W. and Krumlauf, R. (1992). Homeobox genes and axial patterning. *Cell* **68**, 283-302.

Milaire, J. (1967). Histological observations on the developing foot of normal oligosyndactylous (Os/+) and syndactylous (Sm/Sm) mouse embryos. *Archs. Biol. Liège* **78**, 223-288.

Morgan, B.A., Izpisua-Belmonte, J.C., Duboule, D. and Tabin, C. (1992). Targeted misexpression of *Hox-4.6* in the avian limb bud causes apparent homeotic transformations. *Nature* **358**, 236-239.

Mortlock, D. P., Post, L. C. and Innis, J. W. (1996). The molecular basis of Hypodactyly (Hd): a deletion in *Hoxa-13* leads to arrest of digital arch formation. *Nature genet*. **13**, 284-289.

Müller, G.B. (1991). Evolutionary transformation of limb pattern: heterochrony and secondary fusion. In *Developmental Patterning of the Vertebrate Limb* (ed. J.R. Hinchcliffe, J.M. Hurle and D. Summerbell). pp 395-405. New York: Plenum Publishing Corp.

Muragaki, Y., Mundlos, S., Upton, J. and Olsen, B. R. (1996). Altered growth and branching patterns in synpolydactyly caused by mutations in HOXD13. *Science* **272**, 448-451.

Olson, E.N., Arnold, H.-H., Rigby, P.W.J. and Wold, B.J. (1996). Know your neighbors: three phenotypes in null mutants of the myogenic bHLH gene MRF4. *Cell*, **85**, 1-4.

Parr, B.A. and McMahon, A.P. (1995). Dorsalizing signal Wnt-7a required for normal polarity of D-V and A-P axes of mouse limb. *Nature* **374**, 350-353.

Peterson, R.L., Papenbrock, T., Davda, M.M. and Awgulewitsch, A. (1994). The murine HOXC cluster contains five neighboring AbdB-related Hox genes that show unique spatially coordinated expression in posterior embryonic subregions. *Mech. Dev.* **47**, 253-260.

Raynaud, A. and Clergue-Gazeau, M. (1986). Identification des doigts réduits ou manquants dans les pattes des embryons de lézard vert (Lacerta viridis) traités par la cytosine-arabinofuranoside. Comparaison avec les réductions digitales naturelles des espèces de reptiles serpentiformes. *Arch. Biol*. **97**, 279-299.

Riddle, R.D., Johnson, R.L., Laufer, E. and Tabin, C. (1993). Sonic hedgehog mediates the polarizing activity of the ZPA. *Cell* **75**, 1401-1416.

Rijli, F.M., Dollé, P., Fraulob, V., LeMeur, M. and Chambon, P. (1994). Insertion of a targeting construct in a Hoxd-10 allele can influence the control of Hoxd-9 expression. *Dev. Dynamics* **201**, 366-377.

Rine, J. and Herskowitz, I. (1987). Four genes responsible for a position affect on expression from HML and HMR in Saccharomyces cerevisiae. *Genetics* **116**, 9-22.

Shubin, N.H. (1991). The implications of the bauplan for development and evolution of the tetrapod limb. In *Developmental Patterning of the Vertebrate Limb* (ed. J.R. Hinchcliffe, J.M. Hurle and D. Summerbell). pp 411-422. New York: Plenum Publishing Corp.

Shubin, N.H. and Alberch, P. (1986). A morphogenetic approach to the origin and basic organization of the tetrapod limb. *Evol. Biol.* **20**, 319-387.

Small, K.M. and Potter, S.S. (1993). Homeotic transformations and limb defects in Hoxa-11 mutant mice. *Genes Dev*. **7**, 2318-2328.

Sordino, P., van der Hoeven, F. and Duboule, D. (1995). Hox gene expression in teleost fins and the origin of vertebrate digits. *Nature* **375**, 678-681.

Stearns, T. and Botstein, D. (1988). Unlinked noncomplementation: Isolation of new conditional-lethal mutations in each of the tubulin genes of Saccharomyces cerevisiae. *Genetics* **119**, 249-260.

Thomas, K.R. and Capecchi, M.R. (1987). Site-directed mutagenesis by gene targeting in mouse embryo-derived stem cells. *Cell* **51**, 503-512.

Yokouchi, Y., Sasaki, H. and Kuroiwa, A. (1991). Homeobox gene expression correlated with the bifurcation process of limb cartilage development. *Nature* **353**, 443-445.

Yokouchi, Y., Nakazato, S., Yamamoto, M., Goto, Y., Kameda, T., Iba, H. and Kuroiwa, A. (1995). Misexpression of Hoxa-13 induces cartilage homeotic transformation and changes cell adhesiveness in chick limb buds. *Genes Dev*. **9**, 2509-2522.

Zappavigna, V., Sartori, D. and Mavilio, F. (1994). Specificity of Hox protein function depends on DNA-protein and protein-protein interactions, both mediated by the homeodomain. *Genes Dev*. **8**, 732-744.

(Accepted 12 July 1996)